Separation and Purification Technology 269 (2021) 118714

Contents lists available at ScienceDirect

Separation and Purification Technology

journal homepage: www.elsevier.com/locate/seppur

Carbon dioxide capture by non-aqueous blend in rotating packed bed reactor: Absorption and desorption investigation

Yushan Wang [a], Yuning Dong [a], Liangliang Zhang [a,*], Guangwen Chu [a], Haikui Zou [a], Baochang Sun [a], Xiaofei Zeng [a,b]

[a] Research Center of the Ministry of Education for High Gravity Engineering and Technology, Beijing University of Chemical Technology, Beijing, 100029, PR China
[b] State Key Laboratory of Organic-Inorganic Composites, Beijing University of Chemical Technology, Beijing, 100029, PR China

ARTICLE INFO

Keywords:
CO_2 capture
Rotating packed bed
Non-aqueous solution
Direct steam stripping process
Regeneration energy

ABSTRACT

Carbon dioxide (CO_2) capture and storage (CCS) is currently the most effective technology to reduce CO_2 emissions, but it has crucial issues of high energy consumption and low mass transfer efficiency in capture process. In this work, 2-amino-2-methyl-1-propanol (AMP), 2-(2-aminoethylamino)ethanol (AEEA), N-methyl pyrrolidone (NMP) tri-solvent blend is used as a novel non-aqueous absorbent for CO_2 capture process in rotating packed bed (RPB) reactor, which is employed to intensify the mass transfer in both absorption and desorption process. The experimental results show that this new method has good absorption performance. When the CO_2 loading of the lean absorbent is 0.035 mol CO_2/mol amine, the CO_2 capture efficiency is still 89% and the overall volumetric mass transfer coefficient (K_Ga) is 2.67 kmol·m^{-3}·h^{-1}·kPa^{-1}. For desorption process, this study adopted the direct steam stripping (DSS) technique to reduce energy consumption. The optimal regeneration energy consumption by DSS of this non-aqueous absorbent in RPB is about 2.46 GJ/ton CO_2, which is 36.6% lower than that in conventional reboiler regeneration process with 30% MEA solution. The results indicate that this new method has the advantages of high efficiency and low energy consumption, exhibiting good industrial application prospect.

1. Introduction

Due to the massive use of fossil fuels including coal, oil, and natural gas in recent decades, carbon dioxide (CO_2) emissions have greatly increased, resulting in greenhouse effect and global warming. By the end of this century, the global temperature will increase by around 3 °C if no effective CO_2 mitigation measures are taken, which will bring catastrophe to human beings [1,2]. Reducing CO_2 emissions has become the common responsibility of all countries in the world. Carbon dioxide capture and storage (CCS) is currently regarded as the most effective technology to reduce CO_2 emissions [3].

At present, CO_2 capture methods are widely studied. Typical technologies include physical adsorption [4], membrane absorption [5,6], cryogenic distillation [7], physical absorption [8,9], and chemical absorption [10–12]. Among them, the chemical absorption method based on aqueous alkanolamine solutions is one of the most widely used technologies in industry. However, due to the high specific heat capacity and evaporation enthalpy of water, a large amount of energy is needed to raise the temperature of the solution and generate stripping water vapor in the regeneration step. CO_2 reacts with alkanolamine absorbent to form stable carbamates in aqueous environment, which leads to a lot of energy to break the chemical bond between CO_2 and absorbent [13], resulting in difficulties in regeneration. Moreover, the aqueous amine solution can cause corrosion to the reactor because of the high operating temperature and the high conductivity of aqueous solution [14]. In brief, using aqueous amine solutions has the disadvantages of high regeneration energy consumption and equipment corrosion [15–17]. Therefore, many scholars have studied the non-aqueous solutions for CO_2 capture to improve the shortcomings of aqueous amine solutions in recent years. They replaced the water in the alkanolamine solutions by some common organic solvents. In view of the high boiling point and low heat capacity, organic solvents, such as dimethyl sulfoxide (DMSO), N-methyl pyrrolidone (NMP), 2-methoxyethanol (2ME) and 2-ethoxyethanol (2EE) [18–21], have great energy saving potential since it will generate less evaporation and consume less heat to raise the temperature of the absorbent compared to the traditional aqueous amine solution. Besides, studies have shown that regeneration can be carried out at

* Corresponding author.
E-mail address: zhll@mail.buct.edu.cn (L. Zhang).

https://doi.org/10.1016/j.seppur.2021.118714
Received 4 February 2021; Received in revised form 25 March 2021; Accepted 31 March 2021
Available online 5 April 2021
1383-5866/© 2021 Elsevier B.V. All rights reserved.

Nomenclature

C_{in}	CO_2 loading in the inlet, mol CO_2/mol amine
C_{out}	CO_2 loading in the outlet, mol CO_2/mol amine
C_p	specific heat capacity, kJ/(kg·K)
G_I	inert gas flow rate, m^3/h
H	Henry's law constant
$H_{steam,in}$	enthalpy of superheated steam before injected into the RPB, kJ/kg
$H_{steam,rec}$	enthalpy of superheated steam recovered after condensation and re-vaporization process, kJ/kg
$\Delta H_{abs,CO2}$	reaction heat, kJ/mol
HTU	height of mass transfer unit, cm
K_Ga	overall volumetric mass transfer coefficient, kmol/(m^3·h·kPa)
K_La	volumetric mass transfer coefficient, s^{-1}
L	liquid flow rate, L/h
N	rotation speed, r/min
P	total pressure, Pa
qm_{CO2}	mass flow rate of CO_2 during the regeneration process, kg/s
$qm_{solvent}$	mass flow rate of the rich solvent, kg/h
$qm_{stream,in}$	mass flow rate of superheated steam injected into the RPB, kg/h
$qm_{stream,rec}$	mass flow rate of superheated steam recovered after condensation and re-vaporization process, kg/h
Q_G	flow rate of stripping steam, m^3/s
Q_L	flow rate of rich solvent, m^3/s
Q_{reac}	reaction heat provided to the rich solvent by preheater, kJ/s
Q_{sen}	sensible heat provided to rich solvent by preheater, kJ/s
Q_{reg}	total regeneration energy required for the DSS process, kJ/g
Q_{pre}	heat supplied by the preheater, kJ/s
Q_{steam}	energy extracted during steam stripping, kJ/s
r_{in}	inner radius of the packing, m
r_{out}	outer radius of the packing, m
S	stripping factor
T_0	temperature of the rich solvent after passing through rich-lean solvent heat exchanger, °C
T_{feed}	temperature of the rich solvent after preheating, °C
y_{CO2}	mole fraction of CO_2 in the gas phase
y_{CO2}*	equilibrium mole fraction of CO_2 in the gas phase
y_{in}	inlet mole fraction of CO_2 in the gas phase
y_{out}	outlet mole fraction of CO_2 in the gas phase
Z	axial length of the packing, m

Greek symbols

η	capture efficiency
φ	regeneration efficiency
χ	the proportion of the stripping steam exiting the RPB that can be recovered after condensation and re-vaporization process.

lower temperatures by using non-aqueous solvents, which is beneficial to reduce the amine loss by evaporation, their thermal and oxidative degradation and the equipment corrosion rate [19,22]. Guo at el. [21] founded that the blends of monoethanolamine (MEA) with glycol ethers (2ME and 2EE) could significantly reduce the energy consumption by about 55% compared with the benchmark aqueous 5.0 M MEA solution. Bougie et al. [23] studied that the non-aqueous MEA solutions in a mixture of ethylene glycol and 1-propanol (EG/PrOH), diethylene glycol monoethyl ether (DEGMEE), and N-methylformamide (NMF), and the results showed that the blend of MEA and DEGMEE had lowest energy consumption, which was 78% lower than the value obtained for the traditional 30 wt% MEA aqueous solution. Lv et al. [24] studied the energy-efficiency of CO_2 capture of 2-amino-2-methyl-1-propanol (AMP) coupled with different activators dissolved in NMP. The experimental results showed that the non-aqueous solution AMP-AEEA ((2-aminoethylamino)ethanol)-NMP exhibited better performance as a CO_2 capture absorbent since the total heat duty of this new type absorbent is half of that of the aqueous MEA solution.

In the current regeneration process for aqueous amine absorbent, water vapor is generated by the reboiler to strip the CO_2 in the absorbent. Then the mixed gas of water vapor and CO_2 flows out from the top of the tower, and flows back into the tower after condensation and separation. But the boiling point temperature of the non-aqueous absorbent is usually high which means there is not enough stripping gas generated when the absorbent is heated at moderate temperature. So the conventional reboiler regeneration (CRR) process is not applicable for non-aqueous absorbent system. Recently, a regeneration process using direct steam stripping (DSS) has been proposed [25]. The novel process has been proved to be able to reduce the regeneration energy. The schematic flow diagram of DSS is shown in Fig. 1. In DSS, the stripping steam is heated to overheated and then directly injected into the desorption tower to strip the CO_2 from the rich absorbent. Then the steam from the stripper is condensed and separated from the CO_2. The condensation of the steam and re-vaporization of the condensed water from the separator can be carried out in an economizer. The condensed

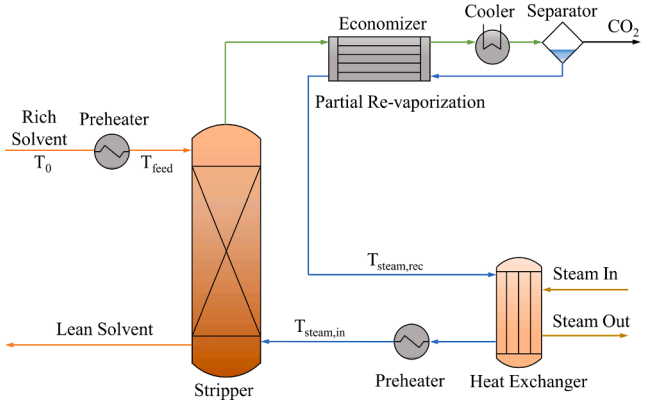

Fig. 1. Schematic flow diagram of DSS.

water can be re-vaporized by utilizing the heat released in condensation process, thereby recovering most of the latent heat effectively. Xiang et al. [26] and Wang et al. [27] investigated the DSS and CRR process through simulations and experiments. And the results proved that the DSS could reduce energy consumption by 20–30% compared to CRR process.

For absorption and desorption process in traditional packed column, the flow of the liquid is driven by gravity field. Therefore, the dispersion and turbulence of the liquid are limited, thereby leading to the inefficiency of mass transfer between gas and liquid phase in traditional reactors. The rotating packed bed (RPB), proposed by Ramshaw and Mallinson [28], can overcome this limitation. In RPB, the packing rotates at high speed, generating strong centrifugal force. And the liquid is dispersed into tiny liquid elements, which increases gas–liquid contact area [29]. Besides, the collision between the liquid and the filler accelerates the renewal rate of the gas–liquid interface [30]. At present,

RPB has been widely used in acid gas capture, such as SO_2 [31,32] and H_2S [33,34]. It has been confirmed that RPB can greatly intensify the gas–liquid mass transfer in these processes.

The purpose of this work is to explore the feasibility of using AMP-AEEA-NMP non-aqueous blend for CO_2 capture in RPB. Both absorption and desorption performances of non-aqueous blend absorbent in RPB are studied. In the AMP-AEEA-NMP system, AMP is the main absorbent, which has a high cyclic absorption capacity, and due to steric hindrance of amine, it will form unstable carbamates, which is beneficial to the regeneration process [20,21]. As a kind of polar organic solvent replacing water in conventional solution, NMP can not only stabilize the reaction products in non-aqueous absorbent [35,36], but also has the potential to reduce regeneration energy consumption due to its high boiling point of 475.15 K and low heat capacity of 1.6 kJ/(kg·K), which is much smaller than the heat capacity of water, 4.2 kJ/(kg·K). AEEA with two amino groups is used as the absorption accelerator to ensure a high absorption rate of the solution. The use of this non-aqueous blend absorbent can essentially reduce the energy consumption of CO_2 capture [24]. For desorption unit, novel DSS technique is used to solve the problem of stripping steam scarcity in the non-aqueous blend absorbent system. Meanwhile, the gas–liquid mass transfer process of both absorption and desorption is expected to be strengthened by RPB. And the absorbent has a short residence time in RPB, which is beneficial to reduce the solvent loss caused by solvent volatilization, especially in the regeneration process. Absorption experiments investigated the effects of different operating conditions including gas–liquid ratio, rotation speed, gas residence time, lean CO_2 loading and operating temperature on CO_2 capture efficiency and the overall volumetric mass transfer coefficient (K_Ga). The desorption experiments explored the influence of rich solvent flow rate, rotation speed, stripping steam flow rate, steam superheat temperature and rich solvent loading on regeneration efficiency, regeneration energy, the volumetric mass transfer coefficient (K_La) and the height of mass transfer unit (*HTU*). The energy consumption for this process is roughly evaluated based on the experimental data and compared with the traditional method. The research results will provide theoretical support for the industrialization of RPB for CO_2 capture.

2. Experimental section

2.1. Materials

AMP (purity ≥ 95%) and AEEA (purity ≥ 99%) were purchased from Shanghai Macklin Biochemical Co., Ltd., China. NMP (purity > 99%) was obtained from Tianjin Damao Chemical Reagent Factory. The non-aqueous solution is composed of AMP (2.5 mol/L) and AEEA (0.5 mol/L) dissolved in the NMP solution. The physical properties of these solvents are shown in Table S1 of Supporting Information. CO_2 (purity ≥ 99.9%) and N_2 (purity ≥ 99.9%) were purchased from Beijing Ruyuanruquan Technology Co., Ltd., China. HCl solution (0.1 mol/L) was provided by Beijing Chemical Works. Concentrated H_2SO_4 (>95 wt%) was supplied by Beijing Chemical Works and diluted to 1 mol/L solution with deionized water. All chemicals were used without further purification.

2.2. Experimental procedure

2.2.1. Absorption experimental procedure

The experimental setup is shown in Fig. 2. Stainless steel wire mesh is used as the filler for RPB. The specification of packing in RPB is listed in Table 1. Typical CO_2 concentration in coal-fired power plant flue gas is in the range of 10–15%. In this absorption experiment, a mixture containing 14% CO_2 is used to simulate flue gas from coal-fired power plant. N_2 and CO_2 are mixed in a gas mixer with a certain proportion. Then, gas mixture enters the RPB from gas inlet and moves inward from outer edge of packing. At the same time, the absorbent with a total amine concentration of 3.6 mol/L is pumped into RPB from the liquid inlet through the liquid distributor and flows out from the liquid outlet. The mixed gas and the absorbent are in countercurrent contact in RPB to remove CO_2. A portable infrared CO_2 analyzer (GXH-3010E, Beijing Huayun Analytical Instrument Research Institute) is connected to the gas inlet and outlet to measure CO_2 concentration. The CO_2 loading in the solvent is measured and analyzed by adding an excess of dilute H_2SO_4 solution. The key operating conditions of the absorption experiment are listed in Table 2

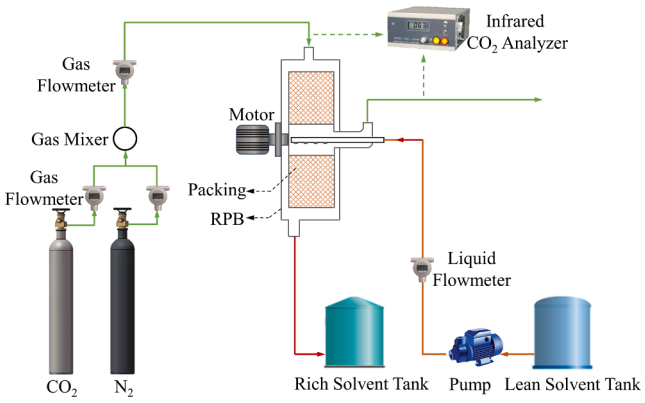

Fig. 2. Schematic diagram of absorption experiment.

Table 1
Specification of packing in RPB.

Item	Value
Inner diameters of the packing, cm	5
Outer diameters of the packing, cm	19
Axial height of the packing, cm	2.3
Special surface area of packing, m^2/m^3	500
Voidage of packing	0.95

2.2.2. Desorption experimental procedure

In this study, DSS process is carried out in RPB to strengthen the regeneration of the non-aqueous solvent. DSS can not only increase the driving force of mass transfer but also reduce energy consumption in the regeneration process.

Fig. 3 is the experimental setup of the desorption experiment. Stainless steel wire mesh is used as the filler for RPB. The specification of packing in RPB is the same as that of the absorption experimental procedure, as shown in Table 1. The rich solvent is prepared by introducing CO_2 into solution with a total amine concentration of 3.6 mol/L. The steam is produced by a steam generator and heated to a predetermined superheating temperature by a heater, and then injected the RPB from the gas inlet. The rich solvent is pumped to the preheater through a peristaltic pump and heated to the required inlet temperature. Then rich solvent enters the RPB from the liquid inlet through the liquid distributor. The rich solvent is in countercurrent contact with the superheated steam in the RPB. The mixed gas of regenerated CO_2 and steam comes out of the RPB from gas outlet and flows into condenser. Samples are taken for analysis when the system is stable. The amine concentration of the mixed amine is measured by an automatic potentiometric titrator (ZDJ-4B, INESA Scientific Instrument Co., Ltd., China). The key

Table 2
The operating conditions of the absorption experiment.

Item	Value
CO_2 inlet concentration	14%
Gas-liquid ratio, L/L	100–260
Rotation speed, r/min	600–1400
Gas residence time, s	0.69–2.08
Lean CO_2 loading, mol CO_2/mol amine	0–0.09
Absorption temperature, K	298.15–333.15
Operating pressure, bar	1

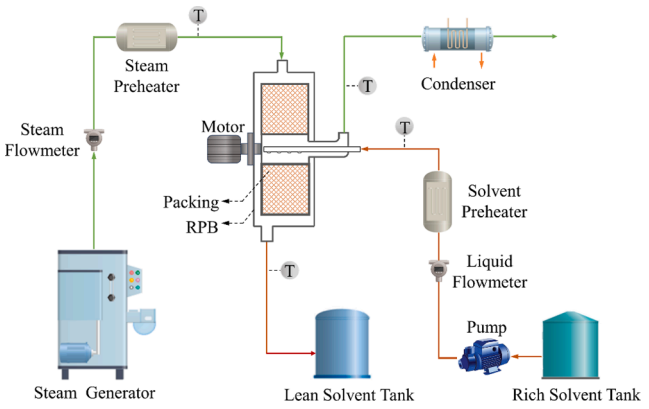

Fig. 3. Schematic diagram of desorption experiment.

operating conditions of the desorption experiment are shown in Table 3.

In the experiment, the flow rate of the rich solvent is 8 to 18 L/h. The rotation speed is adjusted from 800 to 1800 r/min. The stripping steam flow rate is set to 0.6 to 1.4 m^3/h. The steam superheat temperature is controlled in the range of 120 to 140 °C and the loading of the rich solvent is 0.31 to 0.51 mol CO_2/mol amine. All tests are carried out under atmospheric pressure. And samples are taken for analysis when the system is stable. The amine concentration of the mixed amine is measured by an automatic potentiometric titrator (ZDJ-4B, INESA Scientific Instrument Co., Ltd., China).

2.3. Reactions of CO_2 capture with AMP-AEEA-NMP solution

The amines of AMP and AEEA react with CO_2 in NMP. Based on the study of Karlsson et al. [18] and Rayer et al. [37], the reaction between CO_2 and solvent in the absorption process can be described by the following reactions (Eqs. (1)–(8)) according to the zwitterionic mechanism [38,39], where the AMP is denoted by R_1NH_2, AEEA is denoted by R_2NH_2.

In the absence of water, CO_2 reacts with the amines forming the unstable zwitterion.

$$R_1NH_2 + CO_2 \rightleftarrows R_1NH_2^+ COO^- \quad (1)$$

$$R_2NH_2 + CO_2 \rightleftarrows R_2NH_2^+ COO^- \quad (2)$$

Then the zwitterion is protonated to form carbamate in the presence of free amine. The reactions are expressed by Eqs. (3)–(6).

$$R_1NH_2^+ COO^- + R_1NH_2 \rightleftarrows R_1NH_3^+ + R_1NHCOO^- \quad (3)$$

$$R_1NH_2^+ COO^- + R_2NH_2 \rightleftarrows R_1NH_3^+ + R_2NHCOO^- \quad (4)$$

$$R_2NH_2^+ COO^- + R_1NH_2 \rightleftarrows R_2NH_3^+ + R_1NHCOO^- \quad (5)$$

$$R_2NH_2^+ COO^- + R_2NH_2 \rightleftarrows R_2NH_3^+ + R_2NHCOO^- \quad (6)$$

Moreover, the zwitterion can also be rearranged into carbamic acid via intramolecular proton transfer, but the carbamic acid is also unstable and prone to deprotonation by amine molecule to form a carbamate ($RNH_2^+COO^-$ denotes $R_1NH_2^+COO^-$ and $R_2NH_2^+COO^-$, RNH_2 denotes R_1NH_2 and R_2NH_2). The product of carbamic acid makes the 1:1 M ratio of captured CO_2 per amine used in its formation. Meanwhile, NMP as a kind of polar organic solvents can stabilize carbamic acid in non-aqueous solution [36]. Therefore, the loading of AMP-AEEA-NMP system can exceed 0.5 mol CO_2/mol amine.

$$RNH_2^+ COO^- \overset{\text{rearrangement}}{\rightarrow} RNHCOOH \quad (7)$$

$$RNHCOOH + RNH_2 \rightleftarrows RNHCOO^- + RNH_3^+ \quad (8)$$

During the desorption process, the reaction products of CO_2 are regenerated to free amine and free CO_2 under thermal desorption, which is an inverse process of absorption.

2.4. Theoretical method

2.4.1. Data analysis of absorption

The overall volumetric mass transfer coefficient (K_Ga) is an important parameter to evaluate the mass transfer performance in RPB. The understanding of K_Ga can guide the reactor design of absorption process. K_Ga can be calculated by Eq. (9) [40,41].

$$K_Ga = \frac{G_I}{\pi PZ(r_{out}^2 - r_{in}^2)} \int \frac{1}{(y_{CO_2} - y_{CO_2}^*)} d\left(\frac{y_{CO_2}}{1 - y_{CO_2}}\right) \quad (9)$$

where P is total pressure, Z is the axial height of the packing in the RPB. r_{in} and r_{out} represent the inner and outer radii of the packing, respectively. G_I is the inert gas flow rate. y_{CO_2} and $y_{CO_2}^*$ denote mole fraction and equilibrium mole fraction of CO_2 in the gas phase, respectively.

Because the reaction rate between the amine solution and CO_2 is very fast, $y_{CO_2}^*$ can be approximately assumed to be zero. Therefore, K_Ga can be obtained by integrating the Eq. (9).

$$K_Ga = \frac{G_I}{\pi PZ(r_{out}^2 - r_{in}^2)} \times \left[ln\frac{y_{in}(1 - y_{out})}{y_{out}(1 - y_{in})} + \left(\frac{1}{1 - y_{in}} - \frac{1}{1 - y_{out}}\right)\right] \quad (10)$$

where y_{in} and y_{out} are the inlet mole fraction and outlet mole fraction of CO_2 in the gas phase, respectively.

Additionally, the CO_2 capture efficiency η can be calculated by Eq. (11).

$$\eta = \left[1 - \frac{y_{out}(1 - y_{in})}{y_{in}(1 - y_{out})}\right] \times 100\% \quad (11)$$

2.4.2. Data analysis of desorption

The energy requirement of CO_2 regeneration mainly consists of the heat supplied by the preheater and the energy extracted during steam stripping. It can be calculated by the following equation:

$$Q_{reg} = (Q_{pre} + Q_{steam})/qm_{CO_2} \quad (12)$$

where Q_{reg} is total regeneration energy required for the DSS process. Q_{pre} is the heat supplied by the preheater. Q_{steam} is the energy extracted during steam stripping. qm_{CO_2} is the mass flow rate of CO_2 during the regeneration process.

The energy provided by the preheater consists of the sensible heat and reaction heat. It can be calculated by Eq. (13):

$$Q_{pre} = Q_{sen} + Q_{reac} = c_p qm_{solvent}(T_{feed} - T_0) + \Delta H_{abs,CO_2} qm_{CO_2} \quad (13)$$

where Q_{sen} is the sensible heat provided to rich solvent by preheater. Q_{reac} is the reaction heat provided to the rich solvent by preheater. c_p is the specific heat capacity of absorbent [24]. The $qm_{solvent}$ is the mass flow rate of the rich solvent. T_{feed} is the temperature of the rich solvent after preheating. T_0 is an assumed temperature of the rich solvent after passing through rich-lean solvent heat exchanger. In this work, T_0 is set to 85 °C under 1 atm operating pressure [42]. $\Delta H_{abs,CO_2}$ is the reaction

Table 3
The operating conditions of the desorption experiment.

Item	Value
Rich solvent preheat temperature, °C	100
Rich solvent flow rate, L/h	8–18
Rotation speed, r/min	800–1800
Stripping steam flow rate, m^3/h	0.6–1.4
Steam superheat temperature, °C	120–140
Loading of the rich solvent, mol CO_2/mol amine	0.31–0.51
Operating pressure, bar	1

heat of CO_2 with absorbent [24].

Q_{steam} can be calculated by Eqs. (14) and (15):

$$Q_{steam} = H_{steam,in} qm_{steam,in} - H_{steam,rec} qm_{steam,rec} \quad (14)$$

$$qm_{steam,rec} = \chi qm_{steam,in} \quad (15)$$

where $H_{steam,in}$ and $H_{steam,rec}$ are the enthalpy of superheated steam before injected into the RPB and recovered after condensation and re-vaporization process, respectively. $qm_{steam,in}$ and $qm_{steam,rec}$ are the mass flow rate of superheated steam injected into the RPB and recovered after condensation and re-vaporization process, respectively. χ is the proportion of the recovered stripping steam. In previous studies, χ is assumed to be 0.8 for a heat transfer temperature pinch of the economizer is 10–12 K [27].

In addition, the volumetric mass transfer coefficient (K_La) and the height of mass transfer unit (HTU) are of great significance for industrial applications. They were calculated by the following equations [43]:

$$K_La = \frac{Q_L}{\pi Z\left(r_{out}^2 - r_{in}^2\right)} \frac{ln\left[\left(1-\frac{1}{S}\right)\frac{C_{in}}{C_{out}} + \frac{1}{S}\right]}{1-\frac{1}{S}} \quad (16)$$

$$HTU = \frac{(r_{out} - r_{in})\left(1-\frac{1}{S}\right)}{ln\left[\left(1-\frac{1}{S}\right)\frac{C_{in}}{C_{out}} + \frac{1}{S}\right]} \quad (17)$$

$$S = \frac{HQ_G}{Q_L} \quad (18)$$

where Q_L and Q_G are the flow rate of rich solvent and stripping steam, respectively. S is stripping factor, C_{in} and C_{out} are the CO_2 loading in the inlet and outlet liquid, respectively. H is the Henry's law constant, which can be estimated from the literature [20,44].

The regeneration efficiency φ can be calculated by

$$\varphi = \left(1 - \frac{C_{out}}{C_{in}}\right) \times 100\% \quad (19)$$

3. Results and discussion

3.1. Absorption performance investigation

3.1.1. Effects of gas–liquid ratio on CO_2 capture efficiency and K_Ga

Fig. 4 shows the effects of gas–liquid ratio on the CO_2 capture efficiency and K_Ga. The gas–liquid ratio is changed from 100 to 260 L/L by adjusting the inlet absorbent flow rate under a fix gas flow rate of 2 m^3/h. The curve shows that the CO_2 capture efficiency and K_Ga decrease with the increase of gas–liquid ratio. Higher gas–liquid ratio means lower absorbent flow rate, which leads to a smaller distribution of absorption liquid per unit volume of packing and weakens the driving force in the liquid phase. Relatively, the decrease of gas–liquid ratio means a large absorbent flow rate, which increases the gas–liquid contact area and promotes the absorption process. Nevertheless, a smaller gas–liquid ratio represents a larger absorbent circulation, which will lead to an increase in the cost of CO_2 capture. Therefore, an appropriate gas–liquid ratio should be selected according to the CO_2 capture efficiency and absorbent circulation.

3.1.2. Effects of the rotation speed on CO_2 capture efficiency and K_Ga

Fig. 5 presents the effects of the rotation speed on the CO_2 capture efficiency and K_Ga. The centrifugal acceleration can be provided from 274 to 1493 m/s^2 by increasing rotation speed from 600 r/min to 1400 r/min. As shown in the Fig. 5, CO_2 capture efficiency and K_Ga both increase with the increase of rotation speed. Increasing the rotation speed means a greater centrifugal acceleration generated by the rotor in RPB. And the liquid will be split into smaller liquid films, liquid filaments and liquid drops as it passes through the filler at high speed, which increases the gas–liquid contact area. Besides, high-speed rotating packing intensifies the degree of liquid turbulent and increases the update frequency of liquid surface. These factors enhance the mass transfer process. However, a higher rotation speed means a higher motor frequency, which will lead to an increase in energy consumption. Therefore, it is very important to choose a suitable speed for the capture efficiency and energy consumption.

3.1.3. Effects of gas residence time on CO_2 capture efficiency and K_Ga

Fig. 6 shows the dependence of the CO_2 capture efficiency and K_Ga on the gas residence time. In the experiment, the gas residence time is changed by adjusting the gas flow rate under a fixed gas–liquid ratio of 140 L/L. It can be seen from Fig. 6 that CO_2 capture efficiency increases with the gas residence time but K_Ga has an opposite tendency. This is attributed to that increasing the gas flow rate will increase the gas and liquid turbulence degree and decrease the mass transfer resistance, which enhance the gas–liquid mass transfer process. However, the gas residence time decreases with the gas flow rate. As the gas flow rate increases, the gas residence time decreases from 2.08 s to 0.69 s in RPB, causing the absorbent to leave the RPB without a sufficient reaction with the CO_2. Thus the CO_2 capture efficiency decreases with the reduction of gas residence time. Besides, the CO_2 capture efficiency is still above 89% when gas residence time is 0.69 s, indicating RPB has a good operational flexibility to gas flow rate fluctuations.

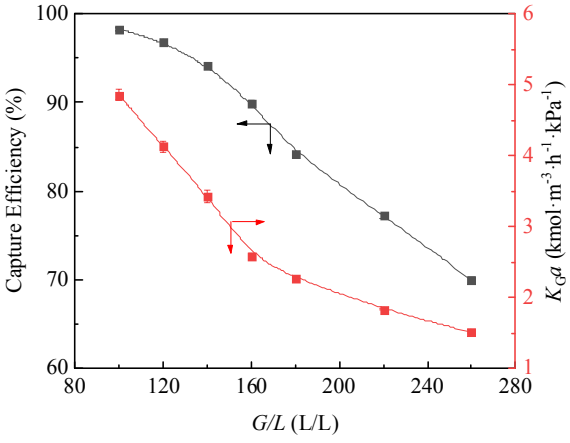

Fig. 4. Effects of gas–liquid ratio on CO_2 capture efficiency and K_Ga (Conditions: G, 2 m^3/h; y_{in}, 14%; N, 1200 r/min; T, 298.15 K; fresh solution).

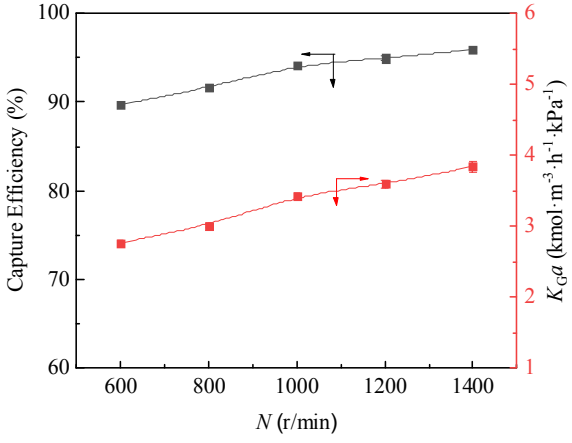

Fig. 5. Effects of the rotation speed on CO_2 capture efficiency and K_Ga (Conditions: G/L, 140 L/L; y_{in}, 14%; T, 298.15 K; fresh solution).

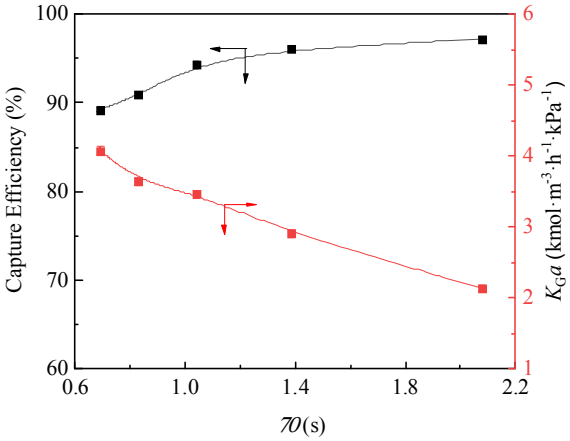

Fig. 6. Effects of gas residence time on CO_2 capture efficiency and K_Ga (Conditions: *G/L*, 140 L/L; y_{in}, 14%; *N*, 1200 r/min; *T*, 298.15 K; fresh solution).

3.1.4. *Effects of lean CO_2 loading on CO_2 capture efficiency and K_Ga*

In actual CO_2 capture process, the absorbent is usually the lean solution with a certain CO_2 loading that is recycled to the absorption unit after regeneration instead of fresh solution. Therefore, it is very necessary to use a lean solution containing a certain CO_2 loading to explore its impact on CO_2 absorption performance. Fig. 7 shows the effects of lean CO_2 loading on the CO_2 capture efficiency and K_Ga. With the increase of lean CO_2 loading, the number of free amino groups in the absorption liquid is reduced, and the mass transfer driving force decreases, which inhibits the transfer of CO_2 molecules to the liquid phase, resulting in the reduction in both CO_2 capture efficiency and K_Ga. When the lean CO_2 loading is 0.035 mol CO_2/mol amine, the CO_2 capture efficiency is still 89% and K_Ga is 2.67 kmol·m^{-3}·h^{-1}·kPa^{-1}. The absorbent with a lean CO_2 loading of 0.058 mol CO_2/mol amine still has a sufficiently fast reaction rate. And the capture efficiency is above 80%. It can be seen that the absorbent has good absorption performance.

3.1.5. *Effects of the temperature on CO_2 capture efficiency and K_Ga*

The temperature of the absorbent is also an important parameter that affects the CO_2 capture efficiency. Fig. 8 shows the effect of absorbent temperature on the CO_2 capture efficiency and K_Ga. The CO_2 capture efficiency and K_Ga increase slightly when the absorbent temperature increases to 303.15 K, but the CO_2 capture efficiency and K_Ga decrease significantly when the temperature exceeds 303.15 K. The increase of absorbent temperature causes the acceleration of molecular motion, improves molecules effective collision and promotes the absorption rate.

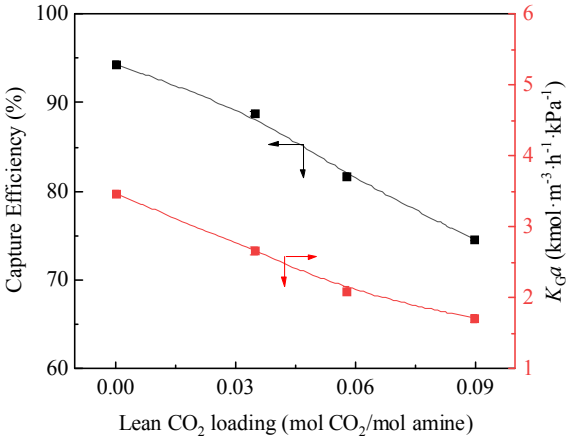

Fig. 7. Effects of lean CO_2 loading on CO_2 capture efficiency and K_Ga (Conditions: *G/L*, 140 L/L; y_{in}, 14%; *N*, 1200 r/min; *T*, 298.15 K).

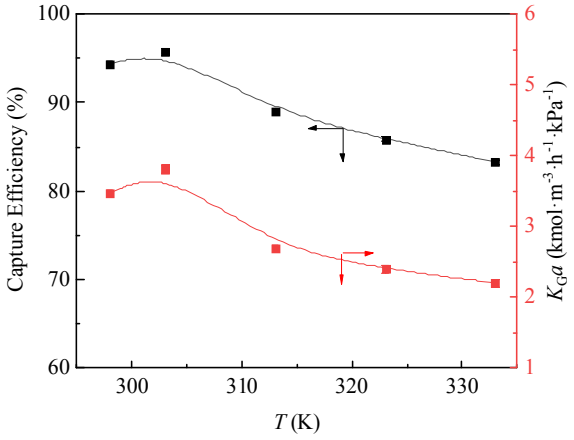

Fig. 8. Effects of the temperature on CO_2 capture efficiency and K_Ga (Conditions: *G/L*, 140 L/L; y_{in}, 14%; *N*, 1200 r/min; fresh solution).

However, when the temperature of the absorbent is higher than 303.15 K, the increase of absorbent temperature reduces the solubility of CO_2 in the absorbent. Meanwhile, as the temperature increases, the reverse reaction rate increases, resulting in the reduction of CO_2 capture efficiency and the decrease of K_Ga. This is related to the characteristics of the main absorbent AMP. The carbamate generated by AMP and CO_2 in non-aqueous solutions is less stable and easily decomposes at higher temperatures [22]. Based on the experimental results, 303.15 K is the optimal absorption temperature of AMP-AEEA-NMP absorbent.

3.2. *Desorption performance investigation*

3.2.1. *Effects of rich solvent flow rate on regeneration performance*

The flow rate of the rich solvent with a loading of about 0.51 mol CO_2/mol amine increased from 8 L/h to 18 L/h. Fig. 9 shows the influence of rich solvent flow rate on regeneration experiment. When the rich solvent flow rate is lower than 14 L/h, the values of regeneration efficiency and K_La increase with the rich solvent flow rate increasing, and the regeneration energy and *HTU* gradually decrease. When the rich solvent flow rate is higher than 14 L/h, although with the increase of the rich solvent flow rate, the mass transfer specific surface area increases and the mass and heat transfer are enhanced, the residence time is shortened, resulting in a gradual decrease in regeneration efficiency, and *HTU* is increased. However, the total amount of CO_2 regenerated increases with the increase of the rich solvent flow rate, so the regeneration energy per unit mass of CO_2 is still a downward trend when the rich solvent flow rate is above 14 L/h. When the rich solvent flow rate is 16 L/h, the minimum energy consumption is 2.46 GJ/ton CO_2. Meanwhile, with the increase of the rich solvent flow rate, the degree of turbulence of gas and liquid increases and the mass transfer resistance decreases, which has a positive impact on the mass transfer coefficient, so that K_La does not significantly decrease when the rich solvent flow rate is higher than 14 L/h.

3.2.2. *Effects of the rotation speed on regeneration performance*

In this study, RPB is used to replace the conventional packed tower for CO_2 regeneration. The rotation speed is a unique operating condition of RPB. Therefore, it is very important to investigate the influence of the rotation speed on the effect of regeneration experiment. The centrifugal acceleration can be provided from 487 to 2468 m/s^2 by increasing rotation speed from 800 r/min to 1800 r/min. Fig. 10 shows the effects of rotation speed on the regeneration experiment. Under the conditions of rich solvent flow rate of 12 L/h, stripping steam flow rate of 1 m^3/h and steam superheating temperature of 130 °C, the regeneration efficiency and K_La increase first and then decrease with the increase of the rotation speed. As the rotation speed increases, the centrifugal force

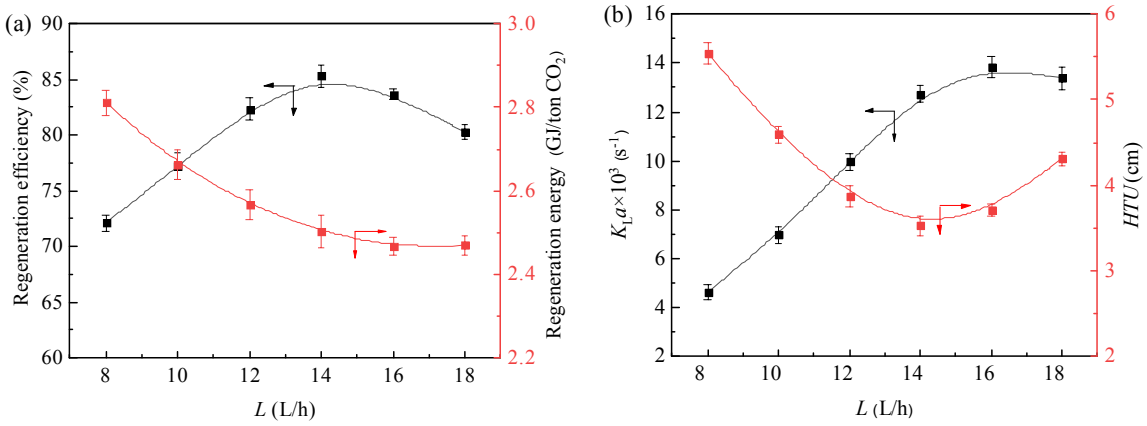

Fig. 9. Effects of rich solvent flow rate on CO_2 desorption ((a): Regeneration efficiency and regeneration energy; (b): K_La and *HTU*) (Conditions: *N*, 1200 r/min; stripping steam flow rate, 1.0 m^3/h; steam superheat temperature, 130 °C; loading of the rich solvent, 0.51 mol CO_2/mol amine).

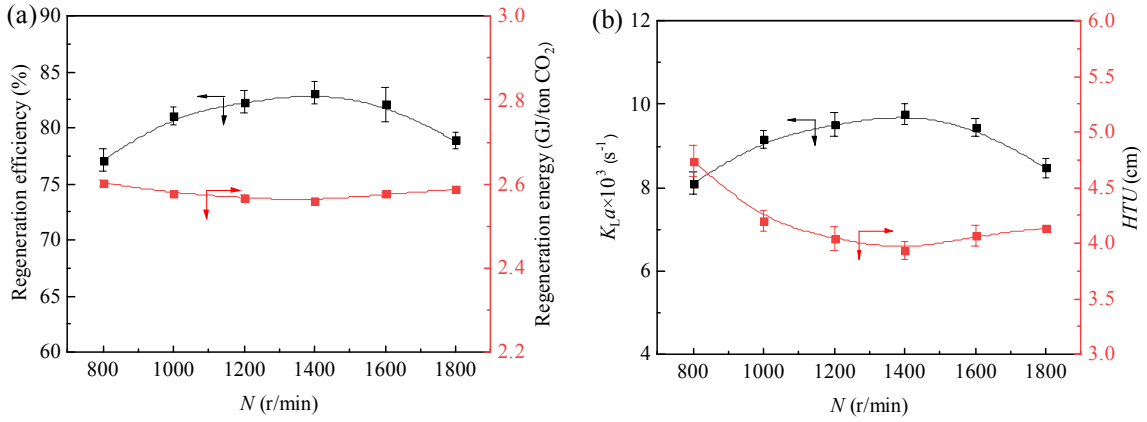

Fig. 10. Effects of the rotation speed on CO_2 desorption ((a): Regeneration efficiency and regeneration energy; (b): K_La and *HTU*) (Conditions: *L*, 12 L/h; stripping steam flow rate, 1.0 m^3/h; steam superheat temperature, 130 °C; loading of the rich solvent, 0.51 mol CO_2/mol amine).

generated by the rotor in the RPB increases, the rich solvent is cut into smaller droplets and thinner liquid film, which increases the gas–liquid contact area. Therefore, the regeneration efficiency and K_La increase with the increase of the rotation speed. However, when the rotation speed is too high, the rich solvent is thrown out of the RPB without enough time for heat and mass transfer, resulting in the decrease of regeneration efficiency and K_La. Correspondingly, the curves of regeneration energy and *HTU* present a downward trend at first and then increase. But the range change of regeneration energy curve is smooth, which indicates that the effect of rotation speed on energy consumption is very small.

3.2.3. *Effects of stripping steam flow rate on regeneration performance*

In this work, DSS replaced the traditional reboiler for stripping, and Fig. 11 shows the effects of adjusting the stripping steam flow rate from 0.6 m^3/h to 1.4 m^3/h on CO_2 regeneration. Stripping steam can provide

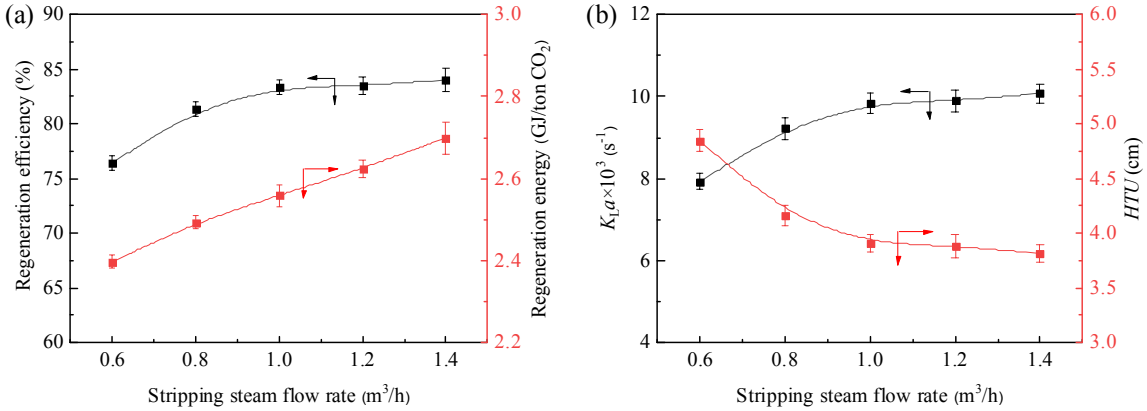

Fig. 11. Effects of stripping steam flow rate on CO_2 desorption ((a): Regeneration efficiency and regeneration energy; (b): K_La and *HTU*) (Conditions: *L*, 12 L/h; *N*, 1200 r/min; steam superheat temperature, 130 °C; loading of the rich solvent, 0.51 mol CO_2/mol amine).

heat to drive the decomposition of carbamate, and direct injection of stripping steam can increase the degree of turbulence of the gas and liquid, and the stripping steam purging can reduce the partial pressure of CO_2 at the phase interface, driving the release of CO_2 from the rich solvent. So the regeneration efficiency and K_La will increase with the stripping steam flow rate rises. But as shown in Fig. 11(a), when the stripping steam flow rate exceeds 1 m^3/h, the regeneration efficiency increases slowly and regeneration energy increases significantly. Fig. 11 (b) shows that as the stripping steam flow rate increases, K_La gradually increases and then tends to be flat, and *HTU* gradually decreases and then tends to be smooth. In the case of a fixed flow rate of the rich solvent, the heat and mass transfer driving forces provided by the smaller stripping steam flow rate are not sufficient to fully regenerate the CO_2 in the rich solvent. Therefore, increasing the stripping steam flow rate can effectively improve the CO_2 regeneration efficiency. When the stripping steam flow rate is large, the heat and mass transfer driving force provided by the stripping steam can regenerate most of the CO_2 in the rich solvent. Therefore, when the stripping steam flow is higher than 1 m^3/h, the CO_2 regeneration efficiency is not obvious enhanced. Based on the results shown in Fig. 11, the optimal stripping steam flow rate of 1 m^3/h is used as the experimental condition.

3.2.4. Effects of steam superheat temperature on regeneration performance

In the desorption process, the stripping steam provides heat for the regeneration of CO_2 in the rich solvent in the experiment, but to avoid the steam condensation during the stripping process, superheated steam is chosen. Therefore, in addition to the flow rate of the stripping steam, the superheat temperature of the steam is also an indicator of the steam characteristics. Fig. 12 shows the effects of increasing the steam superheat temperature from 120 °C to 140 °C on the regeneration experiment in this study. With the increase of steam superheat temperature, the heat provided for the regeneration of CO_2 in the rich solvent gradually increases, and the mass transfer and heat transfer can be enhanced. However, it can be seen from Fig. 12 that the regeneration efficiency and K_La both increase slightly with the steam superheat temperature rises. It proves that increasing the steam superheat temperature has a small promotion effect on CO_2 regeneration. Meanwhile, the enthalpy of superheated steam increases slightly with the increase of superheated temperature, so rising the superheated temperature has little effect on energy consumption.

3.2.5. Effects of rich solvent loading on regeneration performance

The influence of rich solvent loading on regeneration experiment also needs to be investigated. The rich solvent flow rate is 12 L/h, the rotation speed is 1200 r/min, the stripping steam flow rate is 1 m^3/h, and the steam superheat temperature is 130 °C. The rich solvent loading varies from 0.31 mol CO_2/mol amine to 0.51 mol CO_2/mol amine and its influences on the regeneration experiment are shown in Fig. 13. With the increase of the rich solvent loading, the regeneration efficiency and K_La gradually increase. The regeneration energy and *HTU* gradually decrease. When the rich solvent loading is larger, the mass transfer driving force in the system is greater, so as the rich solvent loading increases, the regeneration efficiency and K_La gradually increase. When the rich solvent loading is 0.51 mol CO_2/mol amine, the regeneration efficiency can reach 82%. K_La is 0.009 s^{-1} and *HTU* is only 4 cm, indicating that only a small equipment volume of RPB is required.

3.2.6. Comparison of energy consumption with different regeneration processes

In the CO_2 capture system, the regeneration process has the potential to reduce energy consumption. This work uses the non-aqueous solvent AMP-AEEA-NMP combined with RPB and DSS to reduce regeneration energy. In order to understand these effects on regeneration energy more clearly, regeneration energy is divided into three parts: latent heat, sensible heat and reaction heat. And the regeneration experiment using MEA in RPB combined with DSS process is carried out. The experimental parameters are listed in Supporting Information Table S2. As shown in Fig. 14, the application of DSS process can reduce the latent heat, while the use of RPB can also reduce regeneration energy through enhancing mass and heat transfer. In this work, the regeneration energy of AMP-AEEA-NMP solvent is 2.46 GJ/ton CO_2, which is 36.6% lower than that in CRR process with 30% MEA [26]. The use of the DSS reduces the latent heat by 69.6% compared to the CRR process with 30% MEA. And through the use of AMP-AEEA-NMP absorbent, the sensible heat and reaction heat are reduced by 62.3% and 3.8% respectively compared with using 30% MEA in CRR process. The proposed CO_2 capture method has a good industrial application prospect.

4. Conclusion

This study explored the absorption and desorption processes of CO_2 using a novel non-aqueous absorbent AMP-AEEA-NMP in RPB. Absorption experiments explored the effects of different operating conditions on CO_2 capture efficiency and K_Ga under 14% CO_2 inlet concentration. The experimental results show that the increase of the rotation speed and residence time is beneficial to CO_2 absorption, while increasing gas–liquid ratio is unfavorable to CO_2 capture. And it is not conducive to CO_2 absorption when the absorption solvent temperature exceeds 303.15 K. Although higher lean CO_2 loading is adverse to CO_2 capture, the capture efficiency is still 89% and K_Ga is 2.67 $kmol{\cdot}m^{-3}{\cdot}h^{-1}{\cdot}kPa^{-1}$ when the lean CO_2 loading is 0.035 mol CO_2/mol amine. It shows that the absorbent has good absorption performance. The desorption experiment explored the influence of different operating conditions on regeneration efficiency, regeneration energy, K_La and

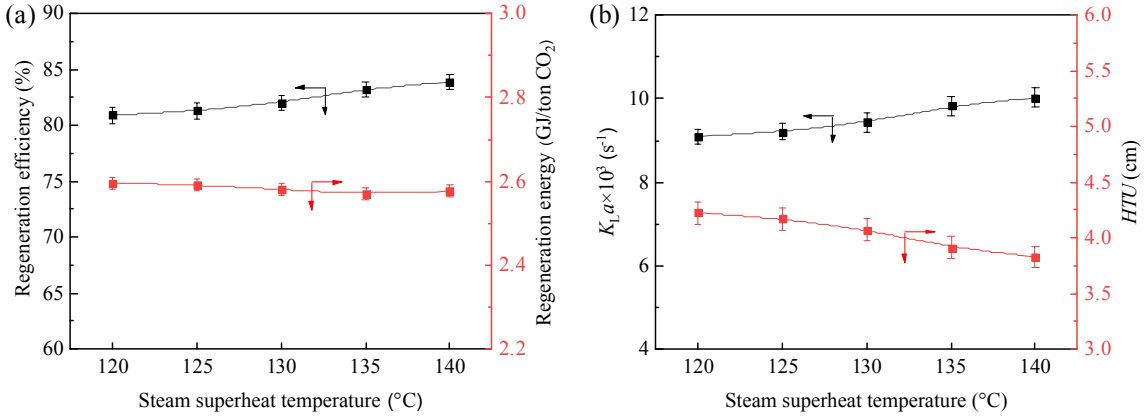

Fig. 12. Effects of steam superheat temperature on CO_2 desorption ((a): Regeneration efficiency and regeneration energy; (b): K_La and *HTU*) (Conditions: *L*, 12 L/h; *N*, 1200 r/min; stripping steam flow rate, 1.0 m^3/h; loading of the rich solvent, 0.51 mol CO_2/mol amine).

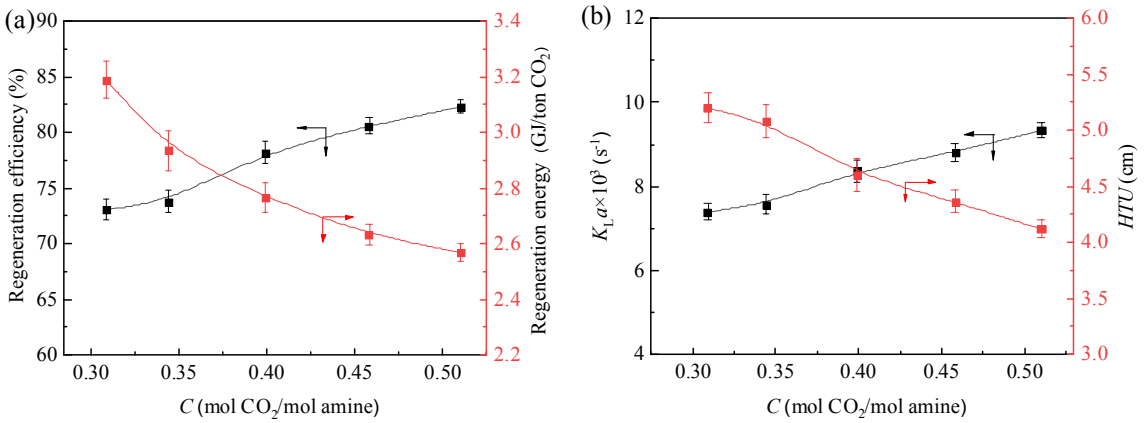

Fig. 13. Effects of rich solvent loading on CO_2 desorption ((a): Regeneration efficiency and regeneration energy; (b): K_La and *HTU*) (Conditions: *L*, 12 L/h; *N*, 1200 r/min; stripping steam flow rate, 1.0 m^3/h; steam superheat temperature, 130 °C).

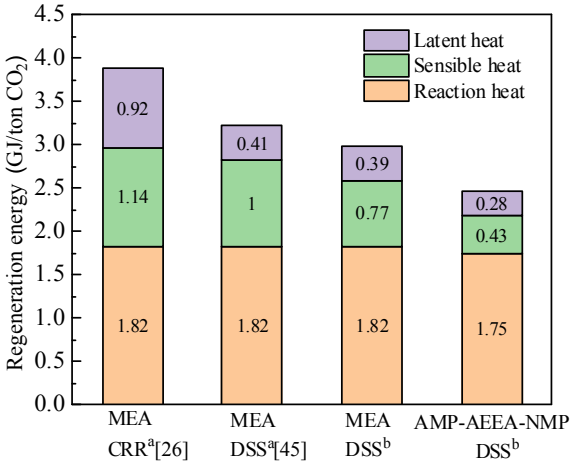

Fig. 14. Comparison of different regeneration processes (a: Regeneration equipment is packing columns [26,45]. b: Regeneration equipment is RPB).

HTU in RPB combined with DSS process. The experimental results show that the increase of rich solvent flow rate, rotation speed, stripping steam flow rate, steam superheat temperature and rich solvent loading all have a positive effect on the CO_2 regeneration efficiency. But the increase of the steam superheat temperature has no significant promotion effect on CO_2 regeneration. And when the value of these conditions exceeds the optimal point, it will have no promotion effect on CO_2 regeneration. In this study, the regeneration energy is 2.46 GJ/ton CO_2 of the non-aqueous solvent AMP-AEEA-NMP combined with RPB and DSS, achieving the reduction of regeneration energy, which is 36.6% lower than that in CRR process with 30% MEA. The DSS used in desorption process can reduce the latent heat compared with CRR. And the use of the non-aqueous absorbent reduces the sensible heat and reaction heat. This study shows that the new method has a good industrial application prospect.

CRediT authorship contribution statement

Yushan Wang: Investigation, Formal analysis, Writing - original draft. **Yuning Dong:** Data curation, Formal analysis, Methodology. **Liangliang Zhang:** Conceptualization, Writing - review & editing, Supervision, Funding acquisition. **Guangwen Chu:** Conceptualization, Resources, Methodology. **Haikui Zou:** Conceptualization, Resources, Methodology. **Baochang Sun:** Resources, Methodology. **Xiaofei Zeng:** Resources, Methodology.

Declaration of Competing Interest

The authors declare that they have no known competing financial interests or personal relationships that could have appeared to influence the work reported in this paper.

Acknowledgements

This work was financially supported by National Key R&D Program of China (No. 2017YFB0603300) and the National Natural Science Foundation of China (Nos. 21978011).

Appendix A. Supplementary material

Supplementary data to this article can be found online at https://doi.org/10.1016/j.seppur.2021.118714.

References

[1] J. Tollefson, Clock ticking on climate action, Nature 562 (2018) 172–173.
[2] Y. Xu, R. Veerabhadran, Well below 2 °C: Mitigation strategies for avoiding dangerous to catastrophic climate changes, Proc. Natl. Acad. Sci. U. S. A. 114 (2017) 10315–10323.
[3] N. MacDowell, A. Florin Buchard, J. Hallett, J. Galindo, G.C. Adjiman, S. Williams, P. Fennell, An overview of CO_2 capture technologies, Energ. Environ. Sci. 3 (2010) 1645–1669.
[4] N. Hiyoshi, K. Yogo, T. Yashima, Adsorption characteristics of carbon dioxide on organically functionalized SBA-15, Micropor. Mesopor. Mat. 84 (2005) 357–365.
[5] A. Brunetti, F. Scura, G. Barbieri, E. Drioli, Membrane technologies for CO_2 separation, J. Membr. Sci. 359 (2010) 115–125.
[6] A. Rosli, A.L. Ahmad, S.C. Low, Enhancing membrane hydrophobicity using silica end-capped with organosilicon for CO_2 absorption in membrane contactor, Sep. Purif. Technol. 251 (2020), 117429.
[7] S. Langè, L.A. Pellegrini, P. Vergani, M. Lo Savio, Energy and economic analysis of a new low-temperature distillation process for the upgrading of high-CO_2 content natural gas streams, Ind. Eng. Chem. Res. 54 (2015) 9770–9782.
[8] S.H. Park, S.J. Lee, J.W. Lee, S.N. Chun, J.B. Lee, The quantitative evaluation of two-stage pre-combustion CO_2 capture processes using the physical solvents with various design parameters, Energy 81 (2015) 47–55.
[9] S. Yang, Y. Qian, S.Y. Yang, Development of a full CO_2 capture process based on the rectisol wash technology, Ind. Eng. Chem. Res. 55 (2016) 6186–6193.
[10] R.R. Wanderley, D.D.D. Pinto, H.K. Knuutila, Investigating opportunities for water-lean solvents in CO_2 capture: VLE and heat of absorption in water-lean solvents containing MEA, Sep. Purif. Technol. 231 (2020), 115883.
[11] F. Bougie, M.C. Iliuta, CO_2 absorption in aqueous piperazine solutions: experimental study and modeling, J. Chem. Eng. Data 56 (2011) 1547–1554.
[12] A. Aboudheir, P. Tontiwachwuthikul, R. Idem, Rigorous model for predicting the behavior of CO_2 absorption into AMP in packed-bed absorption columns, Ind. Eng. Chem. Res. 45 (2006) 2553–2557.
[13] J. Tan, H. Shao, J. Xu, L. Du, G. Luo, Mixture absorption system of monoethanolamine−triethylene glycol for CO_2 capture, Ind. Eng. Chem. Res. 50 (2011) 3966–3976.
[14] J. Li, C.J. You, L.F. Chen, Y.M. Ye, Z.W. Qi, K. Sundmacher, Dynamics of CO_2 absorption and desorption processes in alkanolamine with cosolvent polyethylene glycol, Ind. Eng. Chem. Res. 51 (2012) 12081–12088.

[15] S. Roongrat, A. Adisorn, V. Amornvadee, Behavior of reboiler heat duty for CO_2 capture plants using regenerable single and blended alkanolamines, Ind. Eng. Chem. Res. 44 (2005) 4465–4473.
[16] A. Bello, R.O. Idem, Comprehensive study of the kinetics of the oxidative degradation of CO_2 loaded and concentrated aqueous monoethanolamine (MEA) with and without sodium metavanadate during CO_2 absorption from flue gases, Ind. Eng. Chem. Res. 45 (2006) 2569–2579.
[17] S. Ahn, H.H. Song, J.W. Park, J.H. Lee, I.Y. Lee, K.R. Jang, Characterization of metal corrosion by aqueous amino acid salts for the capture of CO_2, Korean J. Chem. Eng. 27 (2010) 1576–1580.
[18] H.K. Karlsson, P. Drabo, H. Svensson, Precipitating non-aqueous amine systems for absorption of carbon dioxide using 2-amino-2-methyl-1-propanol, Int. J. Greenhouse Gas Control 88 (2019) 460–468.
[19] H.K. Karlsson, H. Makhool, M. Karlsson, H. Svensson, Chemical absorption of carbon dioxide in non-aqueous systems using the amine 2-amino-2-methyl-1-propanol in dimethyl sulfoxide and N-methyl-2-pyrrolidone, Sep. Purif. Technol. 256 (2021), 117789.
[20] H. Svensson, J. Edfeldt, V. Zejnullahu Velasco, C. Hulteberg, H.T. Karlsson, Solubility of carbon dioxide in mixtures of 2-amino-2-methyl-1-propanol and organic solvents, Int. J. Greenhouse Gas Control 27 (2014) 247–254.
[21] H. Guo, C.X. Li, X.Q. Shi, H. Li, S.F. Shen, Nonaqueous amine-based absorbents for energy efficient CO_2 capture, Appl. Energy 239 (2019) 725–734.
[22] F. Barzagli, F. Mani, M. Peruzzini, Efficient CO_2 absorption and low temperature desorption with non-aqueous solvents based on 2-amino-2-methyl-1-propanol (AMP), Int. J. Greenhouse Gas Control 16 (2013) 217–223.
[23] F. Bougie, D. Pokras, X.F. Fan, Novel non-aqueous MEA solutions for CO_2 capture, Int. J. Greenhouse Gas Control 86 (2019) 34–42.
[24] B.H. Lv, K.X. Yang, X.B. Zhou, Z.M. Zhou, G.H. Jing, 2-Amino-2-methyl-1-propanol based non-aqueous absorbent for energy-efficient and non-corrosive carbon dioxide capture, Appl. Energy 264 (2020), 114703.
[25] Y.L. Moullec, M. Kanniche, Screening of flowsheet modifications for an efficient monoethanolamine (MEA) based post-combustion CO_2 capture, Greenhouse Gas Control 5 (2011) 727–740.
[26] Q.Y. Xiang, Y. Le Moullec, M.X. Fang, J.-C. Valle-Marcos, J.H. Lu, W.M. Jiang, X. P. Zhou, G.F. Chen, Z.Y. Luo, Novel solvent regeneration process through direct steam stripping, Energy Procedia 63 (2014) 1392–1398.
[27] T. Wang, H. He, W. Yu, Z. Sharif, M.X. Fang, Process simulations of CO_2 desorption in the interaction between the novel direct steam stripping process and solvents, Energy Fuels 31 (2017) 4255–4262.
[28] C. Ramshaw, R.H. Mallinson, Mass transfer process, in, US (1981).
[29] Y.S. Chen, C.C. Lin, L.H. Shen, Mass transfer in a rotating packed bed with viscous newtonianand non-newtonian fluids, Ind. Eng. Chem. Res. 44 (2005) 1043–1051.
[30] Z. Qian, L.B. Xu, H.B. Cao, K. Guo, Modeling study on absorption of CO_2 by aqueous solutions of n-methyldiethanolamine in rotating packed bed, Ind. Eng. Chem. Res. 48 (2009) 9261–9267.
[31] L.L. Zhang, S.Y. Wu, Y. Gao, B.C. Sun, Y. Luo, H.K. Zou, G.W. Chu, J.F. Chen, Absorption of SO_2 with calcium-based solution in a rotating packed bed, Sep. Purif. Technol. 214 (2019) 148–155.
[32] G.W. Chu, J. Fei, Y. Cai, Y.Z. Liu, Y. Gao, Y. Luo, J.F. Chen, Removal of SO_2 with sodium sulfite solution in a rotating packed bed, Ind. Eng. Chem. Res. 58 (2018) 2329–2335.
[33] J.L. Zhan, B.B. Wang, L.L. Zhang, B.C. Sun, J.W. Fu, G.W. Chu, H.K. Zou, Simultaneous absorption of H_2S and CO_2 into the MDEA + PZ aqueous solution in a rotating packed bed, Ind. Eng. Chem. Res. 59 (2020) 8295–8303.
[34] Z. Qian, Z.H. Li, K. Guo, Industrial applied and modeling research on selective H_2S removal using a rotating packed bed, Ind. Eng. Chem. Res. 51 (2012) 8108–8116.
[35] X.B. Zhou, X.L. Li, J.W. Wei, Y.M. Fan, L. Liao, H.Q. Wang, Novel nonaqueous liquid-liquid biphasic solvent for energy-efficient carbon dioxide capture with low corrosivity, Environ. Sci. Technol. 54 (2020) 16138–16146.
[36] P.V. Kortunov, M. Siskin, L.S. Baugh, D.C. Calabro, In situ nuclear magnetic resonance mechanistic studies of carbon dioxide reactions with liquid amines in non-aqueous systems: evidence for the formation of carbamic acids and zwitterionic species, Energy Fuels 29 (2015) 5940–5966.
[37] A.V. Rayer, A. Henni, J. Li, Reaction kinetics of 2-((2-aminoethyl) amino) ethanol in aqueous and non-aqueous solutions using the stopped-flow technique, Can. J. Chem. Eng. 91 (2013) 490–498.
[38] M. Caplow, Kinetics of carbamate formation and breakdown, J. Am. Chem. Soc. 90 (1968) 6795–6803.
[39] P.V. Danckwerts, The reaction of CO_2 with ethanolamines, Chem. Eng. Sci. 34 (1979) 443–446.
[40] S.Y. Wu, L.L. Zhang, B.C. Sun, H.K. Zou, X.F. Zeng, Y. Luo, Q. Li, J.F. Chen, Mass-transfer performance for CO_2 absorption by 2-(2-aminoethylamino)ethanol solution in a rotating packed bed, Energy Fuels 31 (2017) 14053–14059.
[41] C.X. Xie, Y.N. Dong, L.L. Zhang, G.W. Chu, Y. Luo, B.C. Sun, X.F. Zeng, J.F. Chen, Low-concentration CO_2 capture from natural gas power plants using a rotating packed bed reactor, Energy Fuels 33 (2018) 1713–1721.
[42] M.X. Fang, Q.Y. Xiang, T. Wang, Y. Le Moullec, J.H. Lu, W.M. Jiang, X.P. Zhou, J. B. Zhang, G.F. Chen, Experimental study on the novel direct steam stripping process for postcombustion CO_2 capture, Ind. Eng. Chem. Res. 53 (2014) 18054–18062.
[43] H.H. Cheng, C.C. Lai, C.S. Tan, Thermal regeneration of alkanolamine solutions in a rotating packed bed, Int. J. Greenhouse Gas Control 16 (2013) 206–216.
[44] C. Descamps, Study of the CO_2 capture with physical absorption in an electricity production system based on coal gaseification with an integrated combined cycle, École Nationale Supérieure des Mines de Paris, Eng. Sci. (2004).
[45] J.Y. Yang, W. Yu, T. Wang, Z.Z. Liu, M.X. Fang, Process simulations of the direct non-aqueous gas stripping process for CO_2 desorption, Ind. Eng. Chem. Res. 59 (2019) 7121–7129.